
Received January 30, 2012; reviewed; accepted May 4, 2012

DETERMINATION OF TURBULENCE AND UPPER SIZE LIMIT IN JAMESON FLOTATION CELL BY THE USE OF COMPUTATIONAL FLUID DYNAMIC MODELLING

Oktay SAHBAZ*, Umran ERCETIN, Bahri OTEYAKA*****

*Dumlupinar University, Department of Mining Engineering, Kutahya, Turkey, Tel.: +90 537 3862002;
Fax.: +90 274 2652066; osahbaz@mail.dumlupinar.edu.tr

**Dumlupinar University, Department of Mechanical Engineering, Kutahya, Turkey

***Osmangazi University, Department of Mining Engineering, Eskişehir, Turkey

Abstract. In the coarse particle flotation, turbulence which can be treated as energy dissipation rate, is one of the most significant parameters effecting the recovery and grade. Therefore, determination of energy dissipation rate is very beneficial for delineation of coarse particle flotation and determining the maximum floatable particle size in any cell. In this study, Computational Fluid Dynamic (CFD) modelling for the Jameson cell has been carried out to determine the high turbulent regions and the effect on the upper floatable size limit. The CFD modelling has been utilized for determining the flow characteristics and hydrodynamic behaviour of the Jameson flotation cell. In parallel with this purpose the turbulence map of the cell has been determined and energy dissipation rate determined by using the CFD modelling. According to the result acquired from the CFD modelling, there are two main turbulent regions which are mixing zone in the upper part of the downcomer and critical region at the separation tank. While the high turbulence at the mixing zone supplies fine bubbles and fast collection of particles, the turbulence at the separation tank causes the main detachment of the bubble-particle aggregate. Then, the increase in turbulence in the tank causes the decrease of the maximum floatable size of particles. In addition, the average energy dissipation rate in the critical region has been determined and used for estimation of the maximum floatable particle size in the Jameson cell. Moreover, the effect of hydrophobicity has been discussed.

keywords: Jameson cell, coarse particle flotation, turbulence, CFD modelling

1. Introduction

Flotation is a dynamic process used for separation of hydrophobic minerals from hydrophilic ones. The size of particles is one of the most important parameters in flotation. While the flotation recovery of intermediate particles is high, the recovery of both fine and coarse particles is usually remarkably low (Trahar, 1981). Thus, particle size versus recovery figures leads to the inverted U-shape curves (Trahar, 1981; Nguyen, 2003). The reason of low recovery of coarse particle is mostly the turbulence within the cells (Schulze, 1982; Oteyaka and Soto, 1995; Drzymala,

1994a). Even though particles may have high hydrophobicity, they cannot be reported as a “float” due to the instability of the aggregate as a result of high turbulence. On the other hand, the low recovery of fine particles can be attributed to low collision probability of fine particles (Schulze, 1989; Çinar et al., 2007). Therefore, new and modified conventional technologies are under investigations to increase flotation performance of fine and coarse particles (Rodrigues and Rubio, 2007; Uçurum and Bayat, 2007; Jameson, 2010; Şahbaz, 2010;). Moreover, determination of particle size limits in flotation cells is prepossessed (Nguyen, 2003; Gonjito et al., 2007; Kowalczyk et al., 2011).

The Jameson cell is relatively new flotation device used especially in the flotation of fine particles ($<100\ \mu\text{m}$) with a high performance (Evans et al., 1995; Cowburn et al., 2006; Cinar et al., 2007). However, the collision probability of fine particles increase in the Jameson cell due to the fine bubble ($400\text{-}700\ \mu\text{m}$) generation in the upper part of the downcomer, called the mixing zone, which is one of the main parts of the cell and primary contacting zone of bubble and particle (Evans et al., 1995). On the contrary, the performance of the Jameson cell shows tendency to decrease with the increase of particle size due to turbulence (Cowburn et al., 2006; Cinar et al., 2007). However; due to operational and maintenance issues, it is becoming necessary to recover the coarse particle by using the Jameson cell in existing mineral processing plants (Cowburn et al., 2006). In some applications of coal flotation the feed size can be greater than $500\ \mu\text{m}$ for the Jameson cell (Cowburn et al., 2006). Therefore, the turbulent region causing the detachment should be determined and maximum floatable particle size should be ascertained in the cell.

Computational fluid dynamic (CFD) modelling, which has been recently applied to flotation cells to elucidate complexity of the hydrodynamic characteristics of cells, has been used in flotation science by Koh et al. (2000), Koh and Schwarz (2003 and 2006), Lane et al. (2002), Liu and Schwarz (2009), Sahbaz (2010) etc. In CFD modelling, a flotation cell is discretized into particular finite volumes where local values of flow fields are calculated. The detailed understanding of flows using this approach allows determination of flow characteristics by means of velocity magnitude, pressure changes, turbulence dissipation rate etc. Also this information provides the possibility for investigating where the attachment and detachment occur (Koh et al., 2000; Koh and Schwarz, 2003; 2006). The CFD modelling has become a popular method as it yields informative results and insights to mechanisms, and because of the relatively low labour and equipment costs involved as a result of ever-increasing computer speed and capacity (Liu and Schwarz, 2009). Finally, the CFD modelling seems to be a very useful tool for determination of turbulence, resulting from energy dissipation rate, and related particle size limits in flotation.

In the present study, the turbulence has been quantitatively determined and its effect on the upper particle size limits in the Jameson flotation cell has been ascertained by using the CFD modelling. Furthermore, the effect of particle hydrophobicity on maximum floatable particle size has been elucidated.

2. Material and method

2.1. Material

In the present study high purity quartz ($95\% \pm 1\%$, obtained from Muğla-Milas Region in Turkey) sample was used.

The particle size range of the sample “as received” was $-1+0.5$ mm. The sample was ground in a porcelain mill and sieved for the experiments in different relatively coarser size groups, which are $-150+106$ μm , $-180+150$ μm , $-212+180$ μm , $-250+180$ μm and $-300+250$ μm .

In the experiment, dodecylamine (DDA) was used as a collector. Different amounts of DDA were used to assure required contact angle of 50° and 78° resulting from the 180 g/Mg and 1000 g/Mg DDA, respectively. Aerofroth 65 (AF65) frother, received from Cytec Industries, was added in the form of droplets using a disposable syringe. The amount of AF65 used in the experiments was 10 ppm. The flotation experiments were carried out at natural pH of 8-9 using the domestic tap water.

2.2. Experimental method

The Jameson cell which was used in this study has two main parts, which are “downcomer” with the diameter of 20 mm and “separation tank” with a diameter of 200 mm. The upper part of the downcomer was equipped with a nozzle (Fig. 1) having 4 mm aperture to supply a high pressure water jet and mixing zone at the upper part of the downcomer.

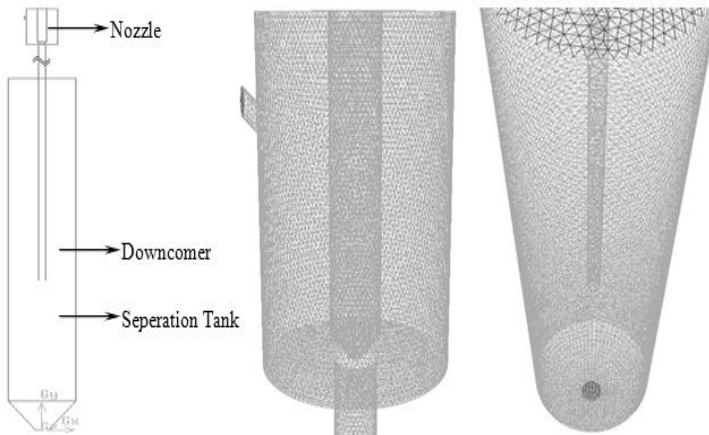


Fig. 1. Meshed view of nozzle, downcomer and separation tank

A conditioned slurry has been pumped (110 kPa) into the downcomer which is the primary contacting zone of particle with bubbles. Air is sucked into downcomer because of the venturi effect of the plunging jet. The sucked air is broken up into fine bubbles produced due to the shearing action of the water jet. Then, micro processes of

flotation, which are encountering, collision, attachment and detachment, start and turbulent region with a high rate occurs at the tip of the nozzle. The three phase mixture is transported into the separation tank due to the gravity flow under high pressure. The second turbulent region occurs at the exit of the downcomer during transportation. This turbulence can be accepted as the turbulence causing the majority of detachment. Therefore, the turbulence, which occurs during the operation must be satisfactorily understood to describe the flotation of coarse particles in the Jameson cell.

During the study all parameters of experiments, such as feeding velocity, solid ratio, air to pulp ratio, have been tried to be kept at optimum conditions considering the previous studies carried out by Evans et al. (1995), Harbort et al. (2002), Çınar et al. (2007), and Sahbaz et al. (2008; 2010).

3. Theory

3.1. The maximum floatable particle size

Flotation of particle depends on the balance of forces acting on bubble-particle aggregate. These forces are the attachment forces between bubble and particle in relation to detachment forces in the environment (Ralston et al., 1999; Pyke et al., 2003; Kowalczyk et al., 2011). The main forces operating at the moment of spherical particle – gas phase rupture are given in Table 1 (Drzymala, 1994b; Pyke et al., 2003; Kowalczyk et al., 2011).

The more realistic force balance for a spherical particle in the liquid/gas interface can be written as in Eq.1 (Kowalczyk et al, 2011):

$$F_{c\max} + F_b + F_h - F_p - F_g - F_a = 0, \quad (1)$$

The sum of the forces is zero at equilibrium. At the equilibrium, particle has the same chance to sink or float. If attachment forces are greater than the detaching forces, particles can float. Therefore; maximum floatable particle size in flotation can be determined by the ratio of the attachment and detachment forces. The probability of stabilisation or destabilisation of the bubble–particle aggregate is based on the Bond number, B_o (Schulze, 1993):

$$B_o = \frac{F_{det}}{F_{att}}, \quad (2)$$

In this equation, the parameter “ a ”, which is used to determine the inertia force, is hard to determine. Additional acceleration, a , determines the detachment forces and depend on the structure and intensity of the turbulent flow field, therewithal on the energy dissipation in a given volume of apparatus (Schulze, 1993). It can be calculated by using the maximum energy dissipation (ε) and aggregate size (D_{agr}) (Pyke et al, 2003):

$$a = 29.6 \frac{\varepsilon^{2/3}}{(D_{agr})^{1/3}}, \tag{3}$$

where aggregate size is

$$D_{agr} = d_b + d_p. \tag{4}$$

Thus, the final equation (5) is obtained to determine the additional acceleration by using Eq. (3) and Eq.(4):

$$a = 29.6 \frac{\varepsilon^{2/3}}{(d_b + d_p)^{1/3}}. \tag{5}$$

In addition, the detachment contact angle, θ_d , in the equations (Table 1) refers to experimental (advancing) contact angle (Kowalczyk et al, 2011).

The maximum floatable size of any particle can be found by using the Bond number calculating the values of forces acting on bubble-particle aggregate by iteration. All terms can be found easily, except for energy dissipation rate, ε , in the cells. The CFD study is one of the useful methods to determine the energy dissipation rate in the flotation cells.

Table 1. Main forces acting on aggregate

Symbol	Force	Equation and Explanation	Effect of force
F_{cmax}	The maximum capillary force	$F_{cmax} = \frac{1}{2} \pi d_{max} \sigma (1 - \cos \theta_d)$ where d_{max} is a maximum floatable particle size, θ_d is a detachment contact angle, and σ is a surface tension	Attachment
F_b	Buoyancy force	$F_b = \frac{1}{8} \pi d_{max}^3 \rho_l g \left(\frac{2}{3} + \cos \frac{\theta_d}{2} - \frac{1}{3} \cos^3 \frac{\theta_d}{2} \right)$ where ρ_l is a liquid density, g is a gravity constant	Attachment
F_h	Hydrostatic pressure force	$F_h = \frac{1}{4} \pi d_{max}^2 (1 - \cos \theta_d) \rho_l g R$ where R is a bubble radius	Attachment
F_p	Pressure in the gas bubble force	$F_p = \frac{1}{4} \pi d_{max}^2 (1 - \cos \theta_d) \frac{\sigma}{R}$	Detachment
F_g	Gravity force	$F_g = \frac{1}{6} \pi d_{max}^3 \rho_p$ where ρ_p is a particle density	Detachment
F_a	Inertia force	$F_a = ma$ $F_a = \frac{1}{6} \pi d_{max}^3 \rho_p a$ where a is an additional acceleration	Detachment

3.2. CFD modelling

The required simulation results for the Jameson flotation system has been numerically modelled using the commercial the CFD code of Fluent. The geometry of the Jameson cell has been defined and a grid has been generated using Gambit 2.4.6 which is the pre-processor for geometry modelling and mesh generation. For all cases studied in this paper, mixtures of triangular and quadrilateral elements have been generated. The computational domain and grid structure in 3D flow field is shown in Fig. 1. The Fluent 6.3.26 commercial computer program for modelling fluid flow, has been used to carry out the modelling of the experimental process. Computations have been performed using Eulerian multiphase approach, for turbulent flows depending on water and air inlet velocity in thr 3D space. The CFD simulations have been performed using a pressure based steady-state segregated implicit solver. A standard k- ϵ mixture model has been employed for flow simulation. Pressure based implicit solver with green-gauss node based has been used. The relationship between velocity and pressure corrections has been calculated using a simple algorithm. A second order upwind discretization scheme has been employed for momentum, turbulent kinetic energy, turbulent dissipation rate and for volume fraction. Gravitational acceleration has been included in the computation and the governing equations for flow and turbulence have been solved iteratively until convergence has been obtained. The inlet velocities of air and water have been entered as 1.4 m/s, volume fraction of air has been set as 43.75%. Outlets have been adjusted as outflow and ratio of the outlets are 20% at mixing outlet and 80% at water outlet. The simulation has been converged after more than 2500 iterations. Grid independence tests for different mesh sizes have been carried out. It was found that the solution has not been affected by the mesh quantity.

4. Results and discussion

The CFD predictions have helped to figure out a complex flow field within the Jameson cell. It has been used to visualize the main turbulent regions within the cell. In addition, values of energy dissipation rates have been determined by the use of the the CFD modelling. Thus, the maximum floatable sizes of particles having contact angles of 50° and 78° have been revealed by the use of the CFD results and the force balance.

The CFD results include turbulence intensity values which indicate that there are two main turbulent regions in the Jameson cell (Fig. 2). It is seen in Fig. 2 that these regions arise from the upper part of the downcomer and at the exit of the downcomer. The turbulence intensity of 1% or less can be considered as low, while the turbulence value greater than 10% can be considered as high (Fluent 6.3 User's Guide). The turbulence intensity at the tip of the nozzle (mixing zone) and downcomer has exceeded the scale and was more than 10% in Fig. 2. But this turbulence may not cause the main detachment because of the compact design and nature of the system.

The high turbulence occurring in the mixing zone is responsible for fine bubble generation (< 1 mm) and faster bubble-particle connection (Evans et al., 1995). In addition to this, detached particles have various chances to attach to bubble again and again along with the downcomer. However, the level of micro-turbulence in the separation tank, as predicted by k-epsilon turbulence model, is highest at the region of the downcomer exit (Fig. 2.). The turbulent region at the exit of the downcomer can be considered as critical region where the main detachment occurs (Harbort et al., 2002; Sahbaz, 2010). The part about 20-25 cm deep from the downcomer exit is the critical part causing the bubble-particle detachment (Fig. 2). Thus, the intensity of turbulent in this critical region in separation tank determines the maximum floatable size of particles (Sahbaz et al., 2010). Turbulence intensity increased to the value of 23% at this region and decreased along with the separation tank (Fig. 2). The degree of intensity finally diminished to less than 1% around the froth phase (upper part) of the separation tank (Fig. 2).

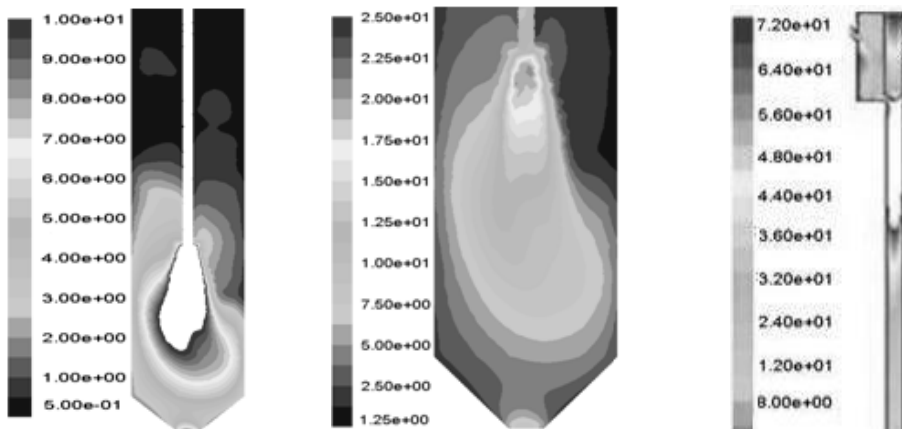


Fig. 2. Contours of turbulence intensity, %

Furthermore, the local turbulent energy dissipation rates are obtained by the CFD modelling of the Jameson cell. The CFD modelling provides a realistic approach to flotation models without additional assumptions on turbulent energy dissipation rates (Evans et al., 2008). Energy dissipation rates obtained from the CFD predictions has also given satisfactory results to comprehend the flow characteristics in the cell (Fig. 3). Furthermore, the value of the energy dissipation rate gives the detachment force acting on bubble particle aggregate within the explicit regions. According to the result obtained from the CFD simulation, the rate of energy dissipation increases at the exit of downcomer and starts to decrease along with the separation tank (Fig. 3). Based on the turbulent dissipation rate, the aggregate stability is mostly disturbed in the separation tank. The local dissipation rate changes between $2.1 \text{ m}^2/\text{s}^3$ and $0.075 \text{ m}^2/\text{s}^3$ (Fig 3). The calculation performed by the use of the exact volume, in which the main detachment zone determined in Fig 4. is about $0.9 \text{ m}^2/\text{s}^3$ (Fig.4-b) according to the

CFD solutions (Fig.4). Thus, the maximum floatable particle size for the laboratory scale Jameson cell can be determined by using this result.

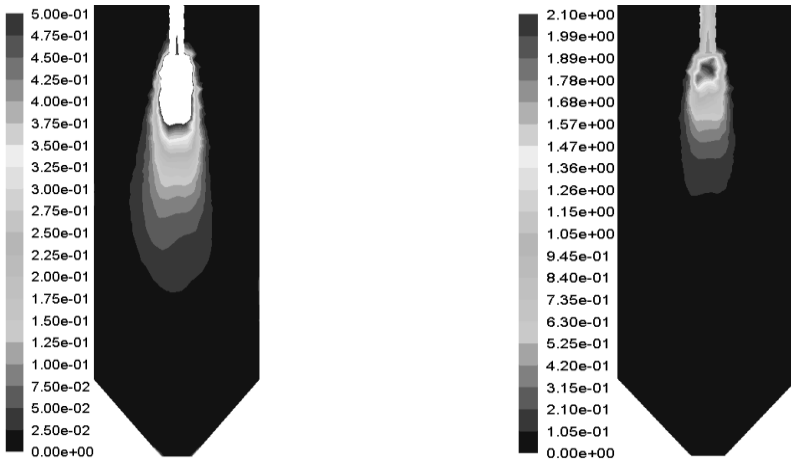


Fig. 3. Energy dissipation rate, m^2/s^3

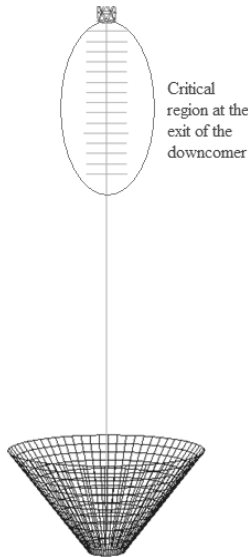


Fig. 4. The critical region determination by the use of the CFD modelling

The relation between theoretical maximum floatable size of particle, d_{max} , and energy dissipation rate is shown in Fig. 5. According to Fig. 5, there is an inverse relation between d_{max} and energy dissipation rate as expected. The figure also shows the same trend for d_{max} having different contact angle values. In addition, Fig. 5 indicates that the capture of large particles is favoured by a low energy dissipation rate

and high contact angles. Finally, theoretical d_{max} for the average dissipation rate have been determined as 260 μm and 345 μm for the contact angle of 50° and 78° , respectively (Fig. 5).

The experimental results which were also published by Şahbaz (2010) are shown in Fig.6. It is seen that the recovery decrease with the particle size increase for both low and high contact angle values (Fig.6). In the same turbulent conditions, the only way of recovery increase of coarse particle is the increase of hydrophobicity. But, even if hydrophobicity is increased, there is still a limitation for floatable particle size. That means that as long as the particle size increases in flotation, the recovery starts to diminish at a critical point. Therefore; there is a d_{max} in every environment and determination of it is beneficial for the operations.

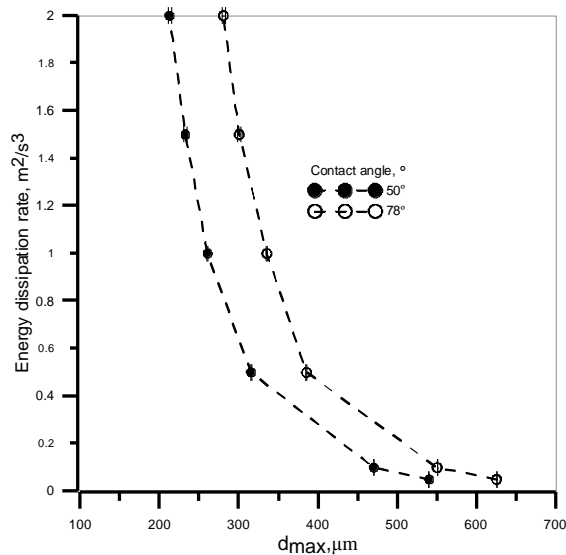


Fig. 5. Relation of d_{max} and energy dissipation rate

d_{max} is defined as the size for which the recovery of floatable particles is equal to 50% (d_{50}). It is a good measure of d_{max} because at that point the particle has equal chance to float and to sink. This was discussed and applied by different authors including Schulze (1977), Drzymala (1994, 1999), Chipfunhu et al. (2011), and Kowalczyk et al. (2011). Therefore, the maximum floatable particle has been found as $235 \pm 20 \mu\text{m}$ and $330 \pm 20 \mu\text{m}$ for the particles having contact angle of 50° and 78° , respectively (Fig. 6).

According to Figs. 5 and 6 there is a close relationship between theoretical and experimental results. Especially these results are nearly the same for the coarser sizes (Figs. 5 and 6). It is possible to speak of a good compliance of high hydrophobicity values between simulation and experimental results (Figs. 5 and 6). It is natural for d_{max} value to increase with the increase of hydrophobicity. Thus, degree of attachments

forces has increased and the recoverable particle size is also increased. However, it can be seen in those figures that there is still a small differences between the experimental and theoretical results for both sizes, specifically for finer ones. The main reason of these differences comes from the difficulty of determination of all detachment regions in the cell. It has been seen that at the turbulent region, particles with a low hydrophobicity are affected more than expected by the model. Bubble-particle aggregate is more prone to detach while passing through the critical region at the exit of the downcomer. This situation causes some differences between CFD simulation results and practical values. As a result, while particles of a size around 250 μm can float in Jameson cell at a low hydrophobicity value; it can reach to 330 μm at a high contact angle value (Figs. 5 and 6).

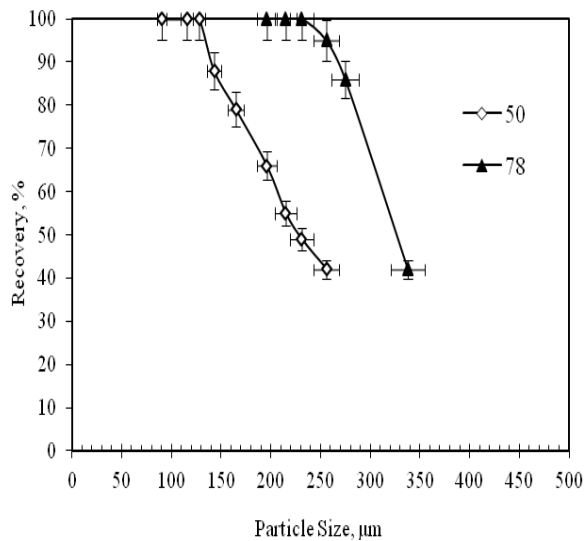


Fig. 6. Experimental results (Şahbaz, 2010)

5. Conclusions

In this study, CFD modelling for the Jameson cell has been carried out to determine the hydrodynamic behaviour and effect of turbulence on the upper floatable size limit. The study shows that there are two main turbulent regions which are mixing zone in the upper part of the downcomer and critical region at the separation tank. While the high turbulence at the mixing zone causes fine bubble generation and fast collection of particle, the turbulence at the separation tank causes the main detachment of the bubble-particle aggregate. Thus, the increase in turbulence in the tank causes the decrease the maximum floatable size of the particle.

According to the CFD simulation the turbulence intensity is higher at the exit of the downcomer than in the whole separation tank. Value of energy dissipation rate within the cell changes between $2.5 \text{ m}^2/\text{s}^3$ and $0.025 \text{ m}^2/\text{s}^3$. In addition to this, the local energy dissipation rate within the critical region is around $0.9 \text{ m}^2/\text{s}^3$. This means that the maximum floatable particle size within the cell is approximately $250 \mu\text{m}$ and $350 \mu\text{m}$ for the contact angle rate of 50° and 78° , respectively. The experimental results have been confirmed by the theoretical results.

Acknowledgement

The authors are thankful to Prof. Dr. Greame J. Jameson for his great support during the design of laboratory scale Jameson cell. And we are also thankful to Dr. Ali Ucar for his advices during the experimental part of this study.

References

- CHIPFUNHU, D., ZANIN, M., GRANO, S., 2011, *Flotation behaviour of fine particles with respect to contact angle*, Chemical Engineering Research and Design, 2011, Article in Press.
- ÇINAR, M., ŞAHBAZ, O., ÇINAR, F., KELEBEK, Ş. AND ÖTEYAKA, B., 2007, *Effect of Jameson cell operating variables and design characteristics on quartz-dodecylamine flotation system*, Minerals Engineering, 20, 1391–1396.
- COWBURN, J., HARBORT, G., MANLAPIG, E. POKRAJCIC, Z., 2006, *Improving the recovery of coarse coal particles in Jameson cell*, Minerals Engineering, 19, 609–618.
- DRZYMALA, J., 1994a, *Characterization of materials by Hallimond tube flotation, Part I. Maximum size of entrained particles*, Int. J. Miner. Process, 42, 139–152.
- DRZYMALA, J., 1994b, *Hydrophobicity and collectorless flotation of inorganic materials*, Adv. Colloid Interface Sci., 50, 143–185.
- EVANS, G.M., ATKINSON, B., JAMESON, G.J., 1995, *The Jameson Cell. Flotation Science and Engineering*, ed. Matis K.A., Marcel Dekker Inc., 331–363.
- EVANS, G.M., DOROODCHI, E., LANE, G.L., KOH, P.T.L., SCHWARZ, M.P., 2008, *Mixing and gas dispersion in mineral flotation cells*, Chemical Engineering Research and Design, 86, 1350–1362.
- FLUENT 6.3 User's Guide, Fluent Inc., Centerra Resource Park, 10 Cavendish Court, Lebanon, NH 03766, USA, 2006.
- GAMBIT User's Guide, Fluent Inc., Centerra Resource Park, 10 Cavendish Court, Lebanon, NH 03766, USA, 2006.
- GONJITO, F.C., Fornasiero, D., Ralston, J., 2007, *The limits of fine and coarse particle flotation*, The Canadian Journal of Chemical Engineering, 85, 739–747.
- HARBORT, G.J., MANLAPIG, E.V. ve DEBONO, S.K., 2002, *Particle collection within the Jameson cell downcomer*, Trans. IMM Section C, 111/Proc. Australas IMM, V. 307.
- JAMESON, G.J., 2010, *New directions in flotation machine design*, Minerals Engineering, 23(11–13), 835–841.
- KOH, P.T.L., MANICKAM, M., M.P. SCHWARZ, 2000, *CFD simulation of bubble-particle collisions in mineral flotation cells*, Minerals Engineering, 13, 1455–1463.
- KOH, P.T.L., SCHWARZ, M.P., 2003, *CFD modelling of bubble-particle collision rates and efficiencies in a flotation cell*, Minerals Engineering, 16, 1055–1059.
- KOH, P.T.L., M.P. SCHWARZ, 2006, *CFD modelling of bubble-particle attachments in flotation cells*, Minerals Engineering, 19, 619–626.
- KOWALCZUK, P., SAHBAZ, O., DRZYMALA, J., 2011, *Maximum size of floating particles in different flotation cells*, Minerals Engineering, 24, 766–771.
- LANE, G.L., SCHWARZ, M.P., EVANS, G.M., 2002, *Predicting gas-liquid flow in a mechanically stirred tank*, Applied Mathematical Modelling, 26, 223–235.

- LUI, T.Y. SCHWARZ, M.P., 2009, *CFD based modelling of bubble particle collision efficiency with mobile bubble surface in a turbulent environment*, International Journal of Mineral Processing, 90, 45–55.
- NGUYEN, A.V., 2003, *New method and equations for determining attachment tenacity and particle size limit in flotation*, International Journal of Mineral Processing, 68, 167–182.
- ÖTEYAKA, B., SOTO, H., 1995, *Modelling of negative bias column for coarse particles flotation*, Minerals Engineering, 8, 91–100.
- ÖTEYAKA, B., 1993, *Modelisation D'une Colonne De Flottation Sans Zone D'écume Pour La Separation Des Particules Grossieres*, PhD Thesis, Université Laval, Quebec, Canada, 1993.
- PYKE, B., FORNASIERO, D., RALSTON, J., 2003, *Bubble particle heterocoagulation under turbulent conditions*, Journal of Colloid and Interface Science, 265, 141–151.
- RALSTON, J., FORNASIERO, D. HAYES, R., 1999, *Bubble-particle attachment and detachment in flotation*, International Journal of Mineral Processing, 56, 133–164.
- RODRIGUES, R.T., RUBIO, J., 2007, *DAF–dissolved air flotation: Potential applications in the mining and mineral processing industry*, International Journal of Mineral Processing, 82, 1–13.
- ŞAHBAZ, O., ÖTEYAKA, B., KELEBEK, Ş., UÇAR A. ve DEMİR, U., 2008, *Separation of unburned carbonaceous matter in bottom ash using Jameson cell*, Separation and Purification Technology, 62, 103–109.
- SAHBAZ, O., 2010, *Modification of downcomer in Jameson Cell and its effect on performance*. Ph.D. Thesis, Dumlupınar University, Department of Mining Engineering, Turkey, 2010.
- SCHUBERT, H., 1999, *On the turbulence-controlled microprocesses in flotation machines*, International Journal of Mineral Processing, 56, 257–276.
- SCHULZE, H.J., 1977, *New theoretical and experimental investigations on stability of bubble/particle aggregates in flotation: a theory on the upper particle size of floatability*, International Journal of Mineral Processing, 4, 241–259.
- SCHULZE, H.J., 1982, *Dimensionless number and approximate calculation of the upper particle size of floatability in flotation machines*, International Journal of Mineral Processing, 9, 321–328.
- SCHULZE, H.J., 1989, *Determination of adhesive strength of particles within the liquid/gas interface in flotation by means of a centrifuge method*, Journal of Colloidal and Interface Science, 128(1).
- SCHULZE, J.H., 1993, *Flotation as a heterocoagulation process: possibilities of calculating the probability of flotation*. Coagulation and Flocculation and Applications. Dekker, New York, ed. Dobias, B., 1993, 321–353.
- TRAHAR, W.J., 1981, *A rational interpretation of the role of particle size in flotation*, International Journal of Mineral Processing, 1981, 8, 289–327.
- UÇURUM, M., BAYAT O., 2007, *Effects of operating variables on modified flotation parameters in the mineral separation*, Separation and Purification Technology, 55 (2), 173–181.